

Development and critical design of magnetic torque rod for low earth orbit satellites

U.Topal^{1,*}, H. Can¹

¹TÜBİTAK-National Metrology Institute, Magnetic Measurements Laboratory, Kocaeli, Türkiye

ARTICLE INFO

Article Type:

Selected Research Article [©]

Article History:

Received: 7 December 2023

Accepted: 11 February 2024

Published: 17 April 2024

Editor of the Article:

M. E. Şahin

Keywords:

Magnetic torque rod, Magnetic torquer, Satellite, Attitude determination and control systems, Magnetic dipole moment, Vibrational tests, Thermal analysis

ABSTRACT

A magnetic torque rod represents an effective means of generating torque for satellite orientation by interacting with Earth's magnetic field. In the dynamic realm of Low Earth Orbit (LEO) satellite systems, precise position control plays a crucial role in the successful execution of a satellite's mission. The insights gained from this study contribute to enhancing the precision, reliability, and diversity of LEO satellite missions, thereby opening doors for new scientific discoveries and technological advancements in Earth observation and beyond. This study delves into critical considerations such as material selection, structural integrity, power consumption and heat management, providing a detailed examination of the fundamental principles behind magnetic torque rod production. To ensure the effectiveness of the torque rod, the design is tailored to the specific dimensions, weight, and power constraints of satellite systems. The designed torque rod possesses a magnetic dipole moment of larger than ± 60 A.m² and consumes just ~ 2.6 Watts of power. Furthermore, it demonstrates the ability to adapt to satellite technology advancements with an operational temperature range of -50°C to $+85^{\circ}\text{C}$.

Cite this article: U. Topal, H. Can, "Development and critical design of magnetic torque rod for LEO satellites," *Turkish Journal of Electromechanics & Energy*, 9(1), pp.3-9, 2024.

1. INTRODUCTION

Attitude determination and control systems (ADCS) play a pivotal role in the operational success of satellites across various space missions. These systems rely on a combination of attitude-determination sensors and actuators, each employing distinct physical principles to achieve their objectives [1]. Notably, ADCS sensors encompass a range of instruments such as horizon sensors, star trackers, sun sensors, and magnetometers, with multiple sensors often employed simultaneously to ensure accuracy and redundancy [2]. Conversely, ADCS actuators include reaction wheels, electrical thrusters, and magnetic torque rods, all of which may be utilized within the framework of a single satellite mission.

Vector magnetometers stand out as particularly critical attitude determination sensors, especially during the initial phases of satellite deployment and orbital stabilization, effectively guiding the satellite to its designated orbit [3, 4]. Other attitude-determination sensors (horizon, star, sun sensors, etc.) are blind and not active in this process. In the same way, the satellite settled in orbit tumbles at random times due to some external factors like solar eruptions. In this case, the satellite cannot again fulfil the mission. It is necessary to stop the tumbling and to provide the

world orientation again. The vector magnetometers, together with the torque rods, take also an active role in this period.

The magnetic torque rod consists of a coil system wound on a rod made of soft ferromagnetic material with high magnetic permeability and saturation magnetization. The structural and magnetic properties of ferromagnetic material are decisive for this equipment to exhibit the expected performance. The production of these cores with such a soft magnetic character and the realization of the necessary heat treatment routines require intellectual experience and are not shared with the scientific community due to economic reasons.

This study aims to design and construct a space-qualified magnetic torque rod suitable for Low earth orbit (LEO) (400-700 km), Medium earth orbit (MEO) (18000-22000 km) and Global positioning system (GPS) missioned satellite systems as an attitude and orientation actuating device. We will explain the design peculiarities for a torquer sample having a linear dipole moment of larger than ± 60 Am², power consumption at 20°C of less than 3 Watt, a residual dipole moment of less than 0.2 Am² and a dipole response time of less than 1 sec. The designed magnetic torquer also allows it to pass environmental tests without loss of performance in the working temperature interval.

[©]Initial version of this article was presented at the 5th International Conference of Materials and Engineering Technology (TICMET'23) held on November 13-16, 2023, in Trabzon, Türkiye. It was subjected to a peer-review process before its publication.

*Corresponding author's e-mail: ugur.topal@tubitak.gov.tr

1.1. Background and Methodology

Assembling a satellite is not an ordinary task. The parts making it up will have to endure aggressive environments like high vacuum, extreme temperatures, radiation and vibration [5]. Therefore, the satellite components undergo rigorous testing long in advance of their mission launch. It is necessary to be cautious at every step while any component is being designed for satellite use. Not paying attention to small details can have serious consequences. For example, outgassing is a major concern in the satellite industry. Vapour coming off plastics, glues and adhesives, as outgassing materials, can deposit on optical devices and/or electronic circuits, thereby degrading their performance. Using ceramic rather than plastic components eliminates this problem in electronics. Besides, soldering remains a vital skill within electronic board assembly. A satellite in low-earth orbit passes from day into night many times a day. This 'thermal cycling' triggers abrupt temperature changes which can induce thermal stress and cracking. All these mean that the building of materials at space qualified form is state of the art. The satellite industry's revenue was reported to be \$208 billion in 2023. With the reason that it has such a huge market, the production stages of the components used in the satellites are not shared with the scientific committee [6].

One of the indispensables of ADCS is magnetic torque rods. Although the magnetic torque rod looks like a simple system consisting of a coil system around a magnetic core, its commercial value is quite high (\$ 100,000-\$ 140,000). They are used mostly in low orbit for discovery and GPS satellites [7]. The reason for the high cost of this equipment is the lack of literature knowledge about its design. Unfortunately, there are no studies in the scientific literature except for a few theoretical articles on torque rod calibration and a few student designs [8, 9]. As a result of the consultations made with relevant institutions about satellite construction, some critical parameters are seen to be important in the torque rod design. Those are mainly dipole moment linearity, saturation moment, residual moment, power and response time.

The behaviour of the magnetic torque rod can be defined by a first-order low-pass filter. The input parameter is the bidirectional drive current and the output is the magnetic dipole moment with unit Am². The magnetic torque rod output parameter varies depending on the input current and the surrounding temperature. One of the other requirements expected from the magnetic torque rod is the restriction in the residual moment. After operating the magnetic torque rod at the maximum moment in the linear region, the residual dipole moment must not exceed 0.3% of the maximum moment. The response time of the magnetic torque rod is another critical parameter to be adjusted. There is a need for two winding systems for backup purposes in magnetic torque rods. When the secondary winding is electrically open, the response time must be less than 100 ms, and if the secondary winding is electrically closed, it must be less than 200 ms. The part that determines the performance and dimensions of the magnetic torque rod seems to be again soft magnetic core. It has a decisive role in critical parameters such as the maximum magnetic moment in the linear region, the power consumption, the response time and the residual magnetic moment. Optimization of these parameters is usually performed after

special heat treatments on nickel, cobalt and iron-based alloys. In the method section of the manuscript, a sample magnetic torque rod design will be explained in detail.

Torque over a dipole placed in a magnetic field B can be formalized as:

$$\tau = m_{dipole} \times B_{ext} \quad (1)$$

From Equation (1), it is seen that there will be no torque if the dipole is parallel to the external field. There must be an angle between the dipole and the field. The satellite orientation is supplied with this principle and turned in the desired direction for the desired angle by driving an adjustable DC to the corresponding magnetic rod. It must noted that the magnetic moment of the rod given in Equation (2) is defined by;

$$m_{tot} = m_{core} + m_{solenoid} = NI(\mu/\mu_0 - 1)A + NIA \quad (2)$$

Here *I* is the driven current, *A* is cross cross-sectional area of the rod, *N* is the total number of winding and μ/μ_0 is the relative permeability of the core. Under normal conditions, each ferromagnetic material has a coercive field and residual magnetization, which is undesirable in this application. For example, the existence of the coercivity causes the torque rod to lose measurement repeatability as well as energy loss. Likewise, the residual magnetization distorts the measurement accuracy. Works on the torque rods focus on eliminating the coercivity and residual magnetization of the core and obtaining a linear *B-H* curve to some extent as seen in Figure 1 [10, 11,12].

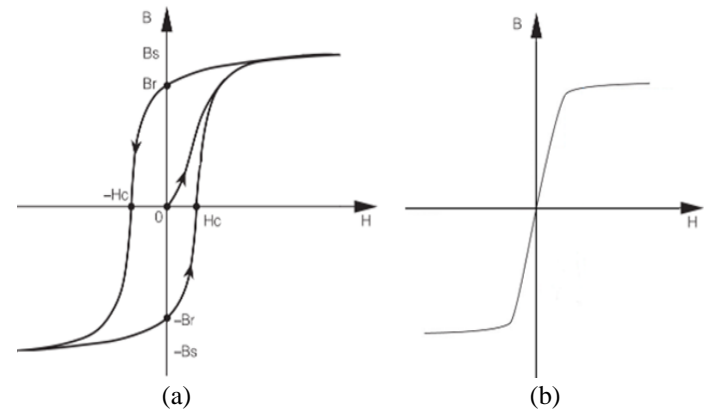


Fig. 1. (a) B-H curve of classical core, (b) B-H curve of the core of torque rod.

Potential materials as the core of the rod must be determined before starting the design. For instance, to satisfy the required dynamical range of $\pm 60 \text{ A.m}^2$, it is necessary to make a rough calculation about the saturation magnetic induction of the core. The targeted rod must generate a magnetic moment of at least 60000 emu ($1 \text{ emu} = 10^{-3} \text{ A.m}^2$). With the restriction on rod dimensions to 30mm x 620 mm (Dia x Length) (together with the winding and the aluminum cover), the maximum size reserved for the core may be 16 mm x 580 mm. It means the core volume can be $\sim 110 \text{ cm}^3$. That is, the moment will be $\sim 545 \text{ emu/ cm}^3$. The minimum required value for the saturation magnetic induction of the selected core was found to be 0.69 Tesla ($630 \text{ emu/ cm}^3 \times 4\pi \times 10^{-4} \text{ T}$) using the conversion of $1 \text{ emu/ cm}^3 = 4\pi \times 10^{-4} \text{ T}$. It is

seen that this value can be reached by CoFe alloys (2.4 T), pure iron (~2.1 T), NiFe alloys (1.6 T) and Mu-metal. On the other hand, one of the parameters that determine the magnetic moment and consequently the dimensions of the torque rod is the magnetic permeability of the core. For the targeted magnetic moment with restrictions on allowed power, the permeability must be at least 100,000 for the ribbon form of the core. For the torque rod dimensions given above, this value is expected to decrease to 2000-3000. Now let's make a simple design. Assume that our design constraints are: mass ≤ 2.0 kg, power ≤ 2.6 watts, voltage = 24 volts, maximum moment = 60 A.m², response time ≤ 1 s and length = 580 mm. First of all, let's find the length of copper wire with given power and voltage as Equation (3).

$$R = \frac{V^2}{P} = \frac{(24 \text{ V})^2}{2.6 \text{ watt}} = 221,538 \Omega \cong 221 \Omega \quad (3)$$

If an enamel-coated wire with a diameter of 200 μm ($R_{\text{Cu}} = 0,538 \Omega / \text{m}$) is used, then the length of the wire must be 410 m. With this length, we can make almost 6500 turns around the core having a diameter of 16 mm. A maximum DC current of 0.108 A can be applied to such a coil ($I_{\text{max}} = P/V = 2,6 \text{ watts} / 24 \text{ volts} = 0,108 \text{ A}$). The most important parameter to be taken into account is the geometric demagnetization factor as given in Equation (4);

$$N_d = \frac{4 \times \left[\ln \left(\frac{l_{\text{rod}}}{r_{\text{rod}}} \right) - 1 \right]}{\left(\frac{l_{\text{rod}}}{r_{\text{rod}}} \right)^2 - \left(4 \times \ln \frac{l_{\text{rod}}}{r_{\text{rod}}} \right)} = \frac{4 \times \left[\ln \left(\frac{58}{0.8} \right) - 1 \right]}{\left(\frac{58}{0.8} \right)^2 - \left(4 \times \ln \frac{58}{0.8} \right)} = 0,003656 \quad (4)$$

If we substitute the demagnetization factor to the magnetic moment formula in Equation (2), then the Equation (5) is obtained;

$$m = \frac{\pi r^2 N I}{\frac{1}{\mu_r} + N_d} = \frac{3.14 \times 0.008^2 \times 6500 \times 0.108}{\frac{1}{\mu_r} + 0.003656} \quad (5)$$

Equation (5) results in a moment of 60 A.m² if the permeability of the core is selected to be 100000. It will be 58 A.m² for a permeability of 10000.

In this calculation, the greatest contribution to the moment comes from the demagnetization factor, which needs to be optimized because it is not possible to play with electrical parameters. Now it is time to calculate the response time of the rod. The response time is known to be $T=L/R$. For a core having a magnetic permeability of 10000, the inductance is obtained by Equation (6).

$$L = \frac{\mu_0 \mu_r N^2 \pi r^2}{l} = \frac{4 \times 3.14 \times 10^{-7} \times 10000 \times 6500^2 \times 3.14 \times 0.008^2}{0,58} \quad (6)$$

Will be 495 H for the wire resistance of 221 Ω . In this condition, the response time is found as 2.2 s. Another important aspect of torque rod studies is the characterization of torque rods. First of all, it is important for measurement accuracy that there must be no magnetic field source or any metal parts containing iron, nickel or cobalt in the vicinity of at least 5 meters inside the

characterization area. First, the coil is driven by DC current. Then, the magnetic field strength is measured by a sensitive magnetometer placed at a distance of two times the length of the torque rod from its centre as shown in Figure 2. Then using Equation (7);

$$m = \frac{4\pi r^3 \Delta B}{\mu_0 \sqrt{1+3\sin^2 \lambda}} \quad (7)$$

the magnetic moment can be determined.

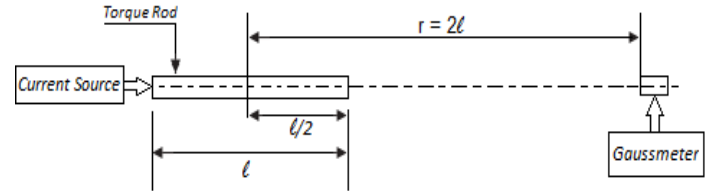


Fig. 2. Measurement setup for the characterization of the designed torque rod.

2. EXPERIMENTAL

As mentioned before magnetic torque rod is an equipment of the satellites that produces magnetic torque over the satellite by interacting with the earth's magnetic field. The general magnetic characteristic of ferromagnetic materials tends to exhibit non-linear behaviour. To ensure a linear relationship between the applied current and the resulting torque the core must be subjected to special heat treatment routines. In the present work, commercially bought nickel and cobalt-based magnetic alloys were chosen as the core of the torque because we need a saturation magnetization of at least 1.5 Tesla to reach a maximum moment of larger than 60 Am². Here, it must be noted that the diameter to the length ratio is quite important for balancing the geometrical demagnetization factor. In our case, the cores having different diameters and lengths were cut from ascast blocks. Then, they were initially annealed under an argon atmosphere for 5 h at 1100 °C and rapidly cooled to 600 °C for 2 hours of annealing. After annealing the ferromagnetic rods, lining with a space-qualified epoxy, obtained from MasterBond Company, was applied to the surface of the rod to avoid short circuits possible during the winding process. For the windings, enamel-coated copper wire with 200 μm diameter was used as shown in Figure 3(a). The torque consists of two windings; one primary and the other backup. Following the winding process, the torque rod is lined with epoxy as in Figure 3(b). The core in wound form is enclosed in an aluminum housing tube as in Figure 3(c) to protect it from radiation and electromagnetic waves. To create a good radiation shield, the wall thickness of the aluminum housing tube is ensured to be at least 2 mm. Additionally, due to the aluminum housing's susceptibility to oxidation or corrosion, black anodization is applied as in Figure 3(d). This treatment enhances the torque rod's surface hardness and improves its resistance to environmental factors. The production stages of the torque rod are shown in Figure 3. All the production process took place in a class 10000 clean room.

3. RESULTS

In this section after making the thermal and vibrational analysis of the designed torque rod, the critical stages of the calibration process will be explained in detail.

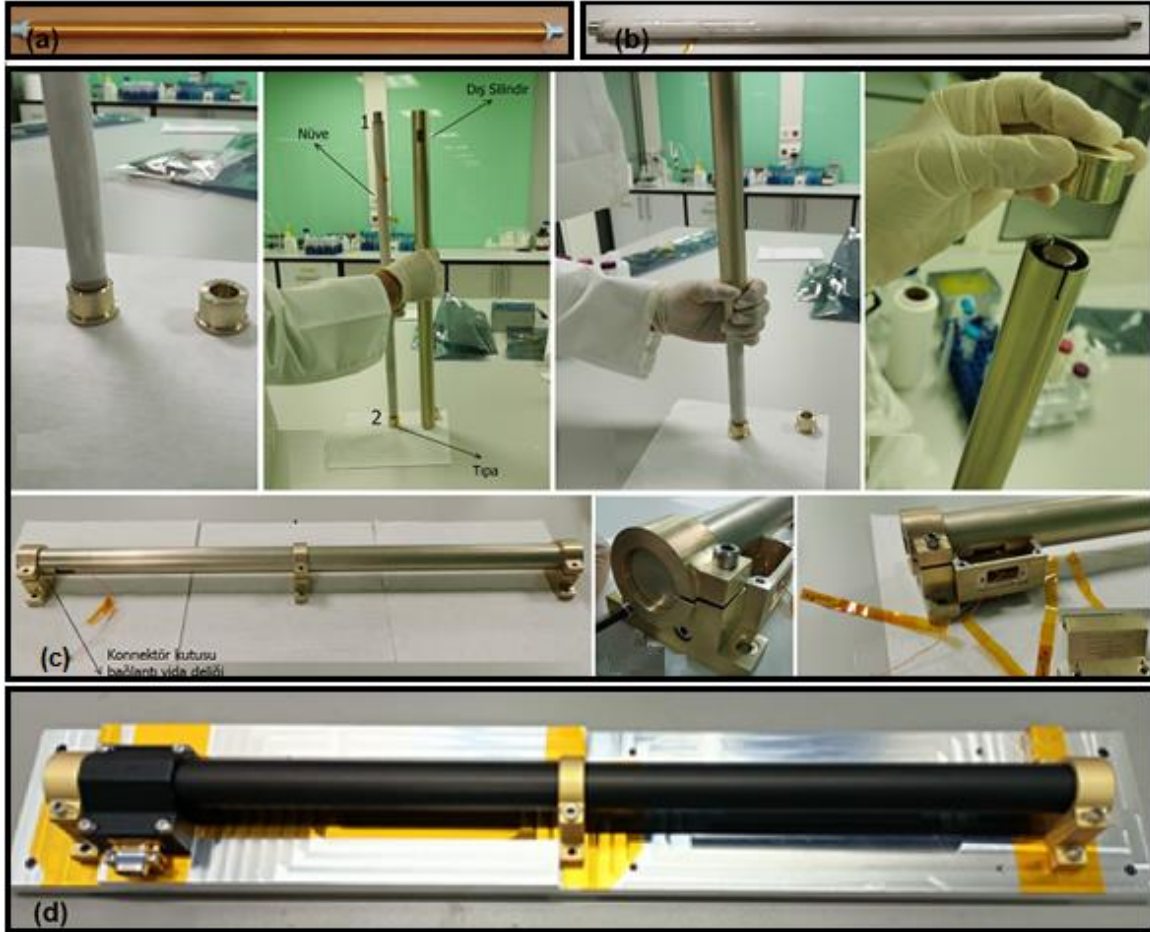


Fig.3. The production stages of the torque rod: (a) Enamel-coated copper wire with 200 μm diameter, (b) The torquer rod lined with epoxy, (c) The core in wound form is enclosed in an aluminum housing tube, (d) Black anodization applied rod.

3.1. Thermal and Vibration Analyses

For any equipment to be used in satellite technologies, it must be able to release the heat generated inside and its eigenfrequencies must not coincide with the eigenfrequencies of the satellite. So, thermal and vibration analysis has a vital role before the fabrication of the equipment.

For this reason, thermal and vibration analysis of the designed device will be discussed in this section. For thermal analysis, the power consumption of each electronic component was calculated and distributed inside the equipment by using the ANSYS program. Figure 4 shows the thermal distribution of the components (the core, aluminium housing, etc.) used in the torquer. As seen in Figure 4(a), the core temperature may rise to 93 $^{\circ}\text{C}$ and remain in equilibrium in case the environmental temperature is 85 $^{\circ}\text{C}$. On the other hand, it just shows 85.4 $^{\circ}\text{C}$ at the endpoints of cylindrical aluminium housing as seen in Figure 4(b). A similar situation is also valid for the ambient temperature of -50 $^{\circ}\text{C}$. At this temperature, the center of the core may rise to -41.1 $^{\circ}\text{C}$ as seen in Figure 4(c), and the edges of the cylindrical housing rise to -49.5 $^{\circ}\text{C}$ as seen in Figure 4(d). This is because the edges of these two components are the unique contact points, and so the heat released by windings, over which the current passes, is thrown out of the device from these contact points.

Companies working in the area of space technologies do not want any equipment with eigenfrequencies below 140 Hz, below

which the equipment can resonate with the frequency of the satellite's main structure. Eigenfrequencies were determined by performing a modal analysis of the magnetic torque rod. As seen from Table 1, the first 10 frequencies are above 140 Hz and provide the requirements. The images corresponding to the 1st, 3rd, 5th, and 7th eigenfrequencies obtained from the analysis are presented from top to bottom in Figure 5. (a) to (d).

Table 1. The first 10 eigenfrequencies of the torque rod were determined from vibration analysis.

Mode	Frequency [Hz]
1	192.08
2	192.57
3	498.36
4	527.43
5	1022.6
6	1025.4
7	1158.1
8	1404.2
9	1568.8
10	1856.4

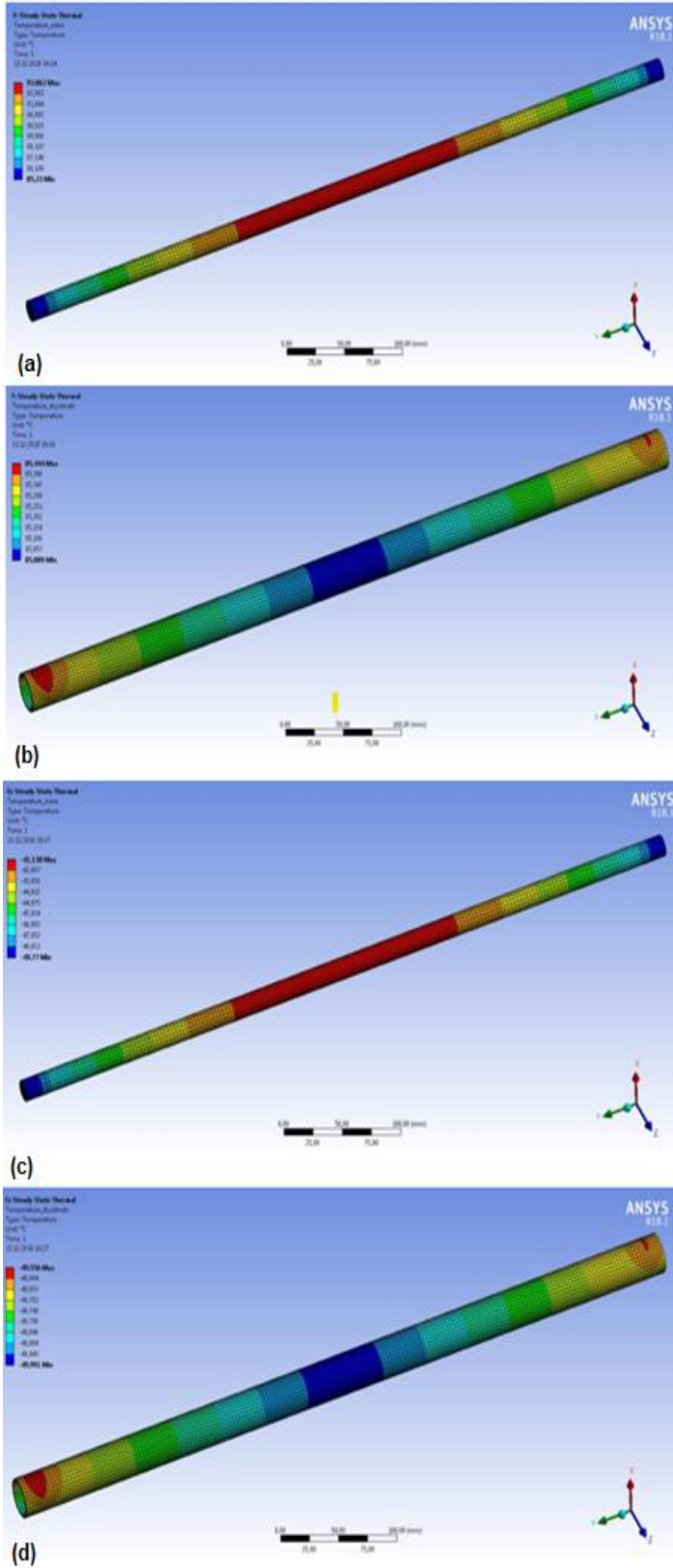


Fig. 4. Thermal analysis of the components forming the torque rod for environmental temperatures of (a) and (b) for 85°C, (c) and (d) for -50 °C.

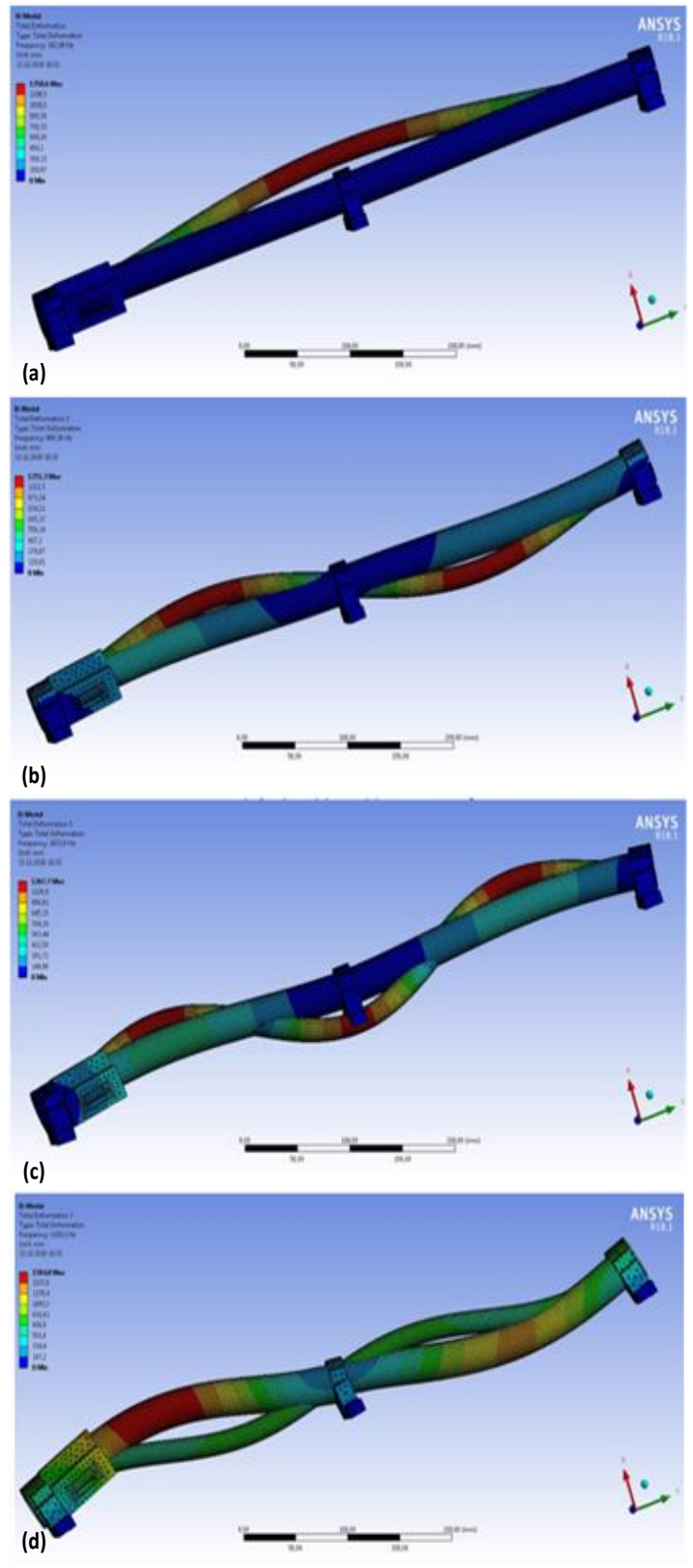


Fig. 5. Vibration analysis of the torque rod for some eigenfrequencies, (a) 1st, (b) 3rd, (c) 5th, and (d) 7th eigenfrequencies.

3.2. Calibration Designed Torque Rod

For the calibration of the magnetic torque rod, a setup shown in Figure 2 was prepared. Keithley 220 current source and LakeShore 450 gaussmeter were used in the measurement system [13, 14]. As seen in Figure 2, the axial probe of the Gaussmeter was placed at a distance twice of torquer's length from the center of it. Initially, both the probe and the rod were placed on a master platform in the same direction. Then, this system was put into a four-layer mu-metal chamber, in which the external earth field was shielded to zero. Magnetic field values were read from the gaussmeter after applying DC current from the current source. In each measurement, the current was first applied and then cut off. The difference in ΔB was measured and noted. Measurements were made in a way to observe potential hysteresis and so, the current is cycled between maximum minus-positive points. In this way, we could determine the residual magnetization values. The magnetic moment value corresponding to each applied current point was calculated using Equation 8.

$$M = \frac{4\pi r^3 \Delta B}{\mu_0 \sqrt{1+3\sin^2\lambda}} \quad (8)$$

Where,

M: magnetic moment ($A.m^2$)

r: the distance of the gaussmeter probe from the center of the torquer rod (m)

ΔB : Change of magnetic field read from the gaussmeter after applying current (T)

μ_0 : Magnetic permeability of free space ($4\pi \times 10^{-7} T.m/A$)

λ : magnetic latitude ($90^\circ - \theta$)

θ : magnetic latitude complement (it is 0° if the position of the magnetic torque rod and the magnetometer relative to each other is parallel, 90° if they are perpendicular).

Figure 6 (a) to (d) shows DC current versus magnetic moment graphs of torque rods with different core compositions, diameters and lengths. From these measurements, it is seen that the number of windings positively affects the torque values. However, winding cannot be increased forever since the ohmic resistance also increases with the number of windings, and this may negatively affect the response time. So, the number of windings needs to be optimized considering both parameters. It is also understood from Figures 6(c) and 6(d) that the core's diameter and length are important. The diameter to length ratio should be reduced as much as possible. It also needs to be optimized according to volumetric requirements. Since the diameter/length ratio also affects the geometric demagnetization factor, magnetic permeability values will take significantly lower values than those of slip geometries. This negatively affects the magnetic moment value to be obtained per unit current. The composition of the chosen magnetic core composition, i.e. magnetic parameters, is important. It seems that a Ni-based composition is more appropriate than a Co-based one for the present purpose. A higher magnetic moment can be reachable with this alloy. In addition, the residual moment formed after the maximum current values, driven between $-$ and $+$, is well below $1.0 A.m^2$ for the nickel alloy. On the other hand, if CoFeV is used, the residual moment becomes around $2.0 A.m^2$.

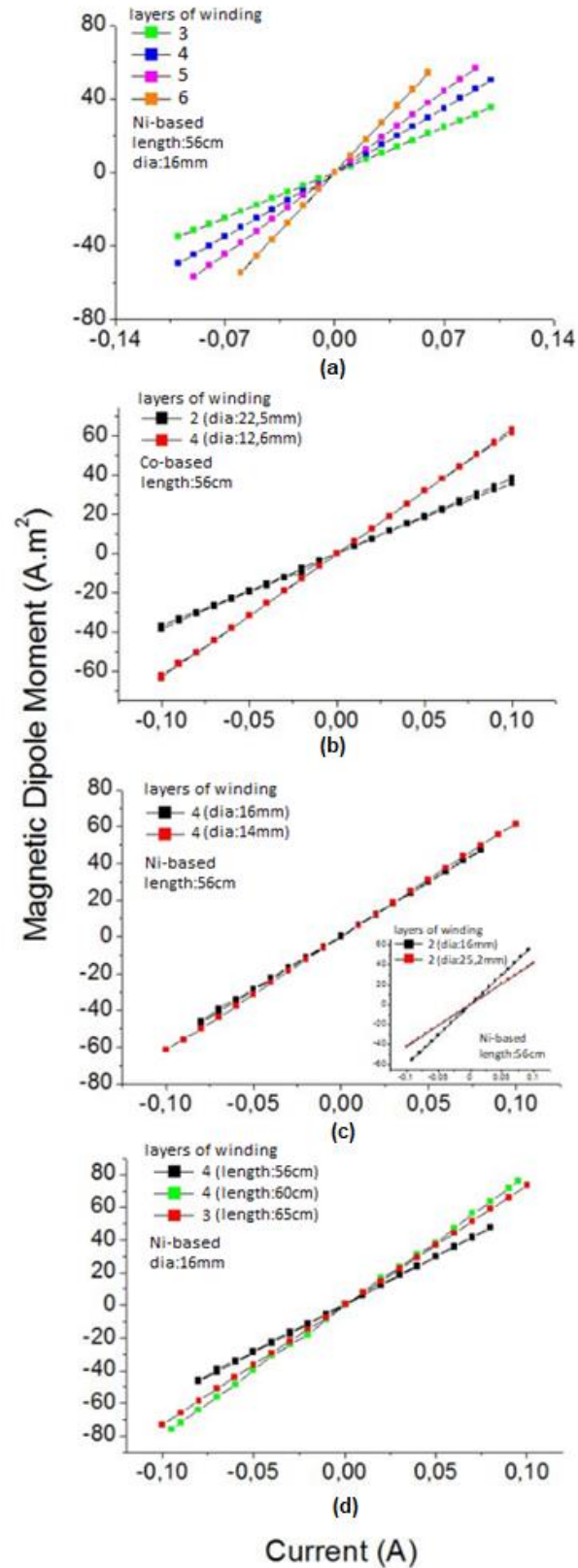


Fig. 6. DC current versus magnetic moment graphs of torque rods with different compositions, diameters and lengths. (a) and (b) for different alloy compositions and the layers of windings (c) the core diameters (d) the core lengths.

Finally, response time measurements were carried out in these core series. Figure 7 (a) shows the response time images of the torque rod for loading and unloading operations in case of 100 mA DC current application. These images given in Figure 7 (b) were obtained from a nickel-based alloy having a diameter of 16 mm and a length of 560 mm. A 1 Ω component resistor was connected in series to this two-winding coil system and the voltage over it was measured via an oscilloscope. From these curves, the time constant, known as Γ , was calculated as approximately 40 ms, and the time required to reach the maximum moment (response time) was calculated as $4\Gamma=160$ ms.

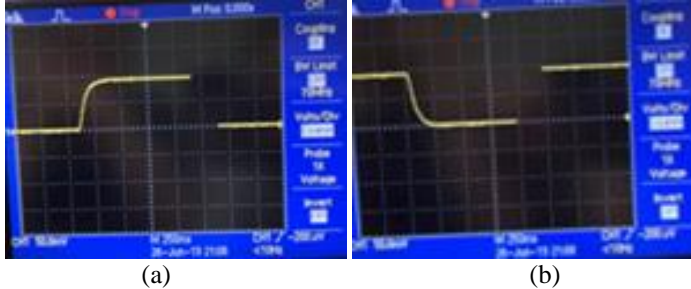


Fig. 7. Oscilloscope images of response time measurements in case of (a) loading and (b) unloading of 100 mA DC current.

4. CONCLUSION

This study reports some critical points of a magnetic torque rod to be used in satellites. Possible magnetic cores and their physical properties were discussed over a sample design. The effects of parameters such as the length, the diameter and the number of windings of the cores on the linearity of the current-moment curves; the maximum torque that can be achieved within power constraints, irreversibility and response time were examined. It has been concluded that the targeted 60 Am² moment and response time under 1 sec. for the existent restrictions can be achieved with two layers (or more) of copper wire 200 μ m diameter wrapped around the Ni-based alloy having a diameter of 16 mm and a length of 560 mm.

References

- [1] T. Bak, "Spacecraft attitude determination: a magnetometer approach," Ph.D. Thesis, Aalborg Univ., Aalborg, Denmark, 1999.
- [2] H. Can, and U. Topal, "Design of ring core fluxgate magnetometer as attitude control sensor for low and high orbit satellites," *J. Supercond. Novel Magnetism*, vol.28, pp. 1093-1096, 2015.
- [3] ECSS, Space environment Standard, Document Number: ECSS-E-ST-10-04C, Noordwijk, Netherlands, 15 June 2020.
- [4] Å. Forslund, S. Belyayev, N. Ivchenko, G. Olsson, T. Edberg, and A. Marusenkov, "Miniaturized digital fluxgate magnetometer for small spacecraft applications," *Meas. Sci. Technol.*, vol. 19, pp. 015202, 2008.
- [5] J. Lee, A. Ng, and R. Jobanputra "On determining dipole moments of a magnetic torquer-experiments and discussions," *Canadian Aeronautics and Space Journal*, 48(1), pp. 61-67, 2002.
- [6] E. Kulu, "Small launchers-2021 industry survey and market analysis," *74th International Astronautical Congress (IAC 2023)*, Baku, Azerbaijan, 2-6 October 2023.

- [7] A. R. Graham, and J. Kingston, "Assessment of the commercial viability of selected options for on-orbit servicing (OOS)," *Acta Astronautica*, vol. 117, pp. 38-48, 2015.
- [8] M. F. Mehrjardi, and M. Mirshams, "Experimental evaluation of a magnetic torquer rod using an innovative test system," *Proc. SPIE 7522, Fourth international conference on experimental mechanics*, 75221X-2, 2009, Singapore.
- [9] NASA Goddard Space Flight Centre, [Online], Available: <https://nasasearch.nasa.gov/search?query=ADCS+magnetometer&affiliate=nasa&utf8=%E2%9C%93>. [Accessed 27 Oct. 2017].
- [10] D. Norte, "Magnetic noise calculations in the presence of three torque rods for spacecraft applications," *IEEE Symposium on Electromagnetic Compatibility and Signal/Power Integrity*, pp. 237, USA, 12 September 2023.
- [11] A. Phanse, "Design, implementation and comparison of power electronic circuits for current control through 3-torquer coils in a Satellite," *IEEE International Conference on Power Electronics and Drive Systems*, Toulouse, France, 2019.
- [12] O. Gürdoğan, A. E. Aydın, S. C. Başaran, "Multilayered implantable antenna design for biotelemetry communication," *Turk. J. of Electromec. Energy*, 3(1), pp. 27-30, 2018.
- [13] Keithley Corp., "Programmable Current Source 220," *Data Sheet*, [Online], Available: <https://www.testequipmenthq.com/datasheets/KEITHLEY-220-Datasheet.pdf>, [Accessed: March 14, 2024]
- [14] Lake Shore Cryotronics, Inc., "Lakeshore model 450 gaussmeter," *User's Manual (P/N 119-005)*, 13 September 2005, [Online], Available: https://www.lakeshore.com/docs/default-source/product-downloads/450_manual.pdf?sfvrsn=76ed6fcf_1 [Accessed: March 14, 2024].

Biographies



Uğur Topal received his PhD degree in physics in 2003 from Middle East Technical University, Ankara, Turkey. After working as a research assistant at Abant İzzet Baysal University for four years, he joined the National Metrology Institute (UME) of Turkey in 1999. He is still working in UME as a senior chief specialist researcher. His

research interests include the synthesis and characterization of magnetic and superconducting materials, their potential applications in industry, magnetic sensor technologies and functional materials, attitude and control determination sensors and actuators of low orbit satellites.

E-mail: ugur.topal@tubitak.gov.tr



Hava Can receive her PhD degree in physics from the Gebze Technical University, Kocaeli, Turkey, in 2018. She has been serving as a senior specialist researcher at the National Metrology Institute of TÜBİTAK, where she joined in 2017. Her current research interests include fluxgate sensor technologies, attitude and control determination sensors, and actuators of low-orbit satellites.

E-mail: hava.can@tubitak.gov.tr